

See discussions, stats, and author profiles for this publication at: <https://www.researchgate.net/publication/6983249>

Dielectric Response of Imidazolium-Based Room-Temperature Ionic Liquids

ARTICLE *in* THE JOURNAL OF PHYSICAL CHEMISTRY B · JULY 2006

Impact Factor: 3.3 · DOI: 10.1021/jp0604903 · Source: PubMed

CITATIONS

188

READS

98

7 AUTHORS, INCLUDING:



[Corinne Daguenet](#)

DSM Nutritional Products

13 PUBLICATIONS 946 CITATIONS

[SEE PROFILE](#)



[Ingo Krossing](#)

University of Freiburg

315 PUBLICATIONS 5,534 CITATIONS

[SEE PROFILE](#)



[Alla Oleinikova](#)

Technische Universität Dortmund

91 PUBLICATIONS 2,667 CITATIONS

[SEE PROFILE](#)



[Hermann Weingärtner](#)

Ruhr-Universität Bochum

98 PUBLICATIONS 3,786 CITATIONS

[SEE PROFILE](#)

Dielectric Response of Imidazolium-Based Room-Temperature Ionic Liquids

Corinne Daguenet,[†] Paul J. Dyson,[†] Ingo Krossing,[§] Alla Oleinikova,[‡] John Slattery,[§] Chihiro Wakai,[‡] and Hermann Weingärtner^{*,‡}

Physical Chemistry 2, Ruhr-University Bochum, D-44780 Bochum, Germany, Ecole Polytechnique Fédérale de Lausanne, Institut des Sciences et Ingénierie Chimiques, CH-1015 Lausanne, Switzerland, and Institut für Anorganische und Analytische Chemie, Albert-Ludwigs-Universität Freiburg, Albertstrasse 21, D-79104 Freiburg, Germany

Received: January 24, 2006; In Final Form: April 27, 2006

We have used microwave dielectric relaxation spectroscopy to study the picosecond dynamics of five low-viscosity, highly conductive room temperature ionic liquids based on 1-alkyl-3-methylimidazolium cations paired with the bis((trifluoromethyl)sulfonyl)imide anion. Up to 20 GHz the dielectric response is bimodal. The longest relaxation component at the time scale of several 100 ps reveals strongly nonexponential dynamics and correlates with the viscosity in a manner consistent with hydrodynamic predictions for the diffusive reorientation of dipolar ions. Methyl substitution at the C2 position destroys this correlation. The time constants of the weak second process at the 20 ps time scale are practically the same for each salt. This intermediate process seems to correlate with similar modes in optical Kerr effect spectra, but its physical origin is unclear. The missing high-frequency portion of the spectra indicates relaxation beyond the upper cutoff frequency of 20 GHz, presumably due to subpicosecond translational and librational displacements of ions in the cage of their counterions. There is no evidence for orientational relaxation of long-lived ion pairs.

I. Introduction

Imidazolium-based room-temperature ionic liquids (RTILs) form a promising class of environmentally benign solvents with properties that can be tuned by variation of the cation and anion. Such variations can dramatically influence the outcome and rate of chemical reactions.^{1–3} An understanding of these phenomena requires an understanding of the coupling of solvent motions to the chemical reaction dynamics. In this context, there is interest in the dielectric response of the solvent because the rates of reactions involving charge transfer strongly depend on the dielectric friction exerted by the solvent.⁴

In the normal fluid region the major portion of the dielectric response lies at the time scale of picoseconds to nanoseconds probed by microwave spectroscopy. Such microwave experiments are difficult because the samples are largely short-circuited by their intrinsic electrical conductance.^{5,6} In a study of molten ethylammonium nitrate ([EtNH₃]⁺[NO₃][−]) we have demonstrated that these problems can be overcome by careful experiments.⁵ We have also shown that such experiments yield static dielectric constants of RTILs which are not available by conventional methods.⁶ Prior to that work, dielectric spectroscopy of molten salts was limited to glassy systems, where the low conductivity facilitates experimentation.⁷ Meanwhile, such data have also been reported for dibutylammonium formate ([Bu₂NH₂]⁺[Fo][−]) near its glass transition.⁸

Here we report the first systematic application of dielectric relaxation to highly conductive 1-alkyl-3-methylimidazolium

bis((trifluoromethyl)sulfonyl)imides (bis(triflyl)imides) [RMeIm]⁺[Tf₂N][−], where R stands for the ethyl (Et), *n*-propyl (Pr), *n*-butyl (Bu), and *n*-pentyl (Pe) residues (see Chart 1). Bis(triflyl)imides are prototypical examples for hydrophobic, low-viscosity, and thermally stable RTILs.⁹ For comparison, we also consider the 1-butyl-2-methyl-3-methylimidazolium salt ([BuMeMeIm]⁺[Tf₂N][−]), where the acid proton at the C2 carbon of the aromatic imidazolium ring is substituted by a methyl group.

In molten salts consisting of monatomic ions, the dielectric response arises from translational displacements of charges.⁷ In contrast, the permanent dipole moments of the molecular ions open channels for orientational relaxation, as encountered in nonionic fluids. However, the transcription of the well-established dielectric theory of simple dipolar fluids¹⁰ to RTILs is an almost untouched problem.¹¹ In addition, transient dipolar ion pairs may drive relaxation, if they survive at the time scale of molecular reorientation.¹² Such mechanisms are well established for long-lived ion pairs in electrolyte solutions, where dielectric spectroscopy forms a standard tool for studying ion pair relaxation.¹³ For bis(triflyl)imides, the existence of collectively moving ions of opposite charges has been deduced from diffusion and conductance data,¹⁴ but the lifetime of the ion configurations is unknown. There is also some debate on the role of hydrogen bonds between anions and the ring protons of imidazolium cations for the stability of ion pairs.^{15,16}

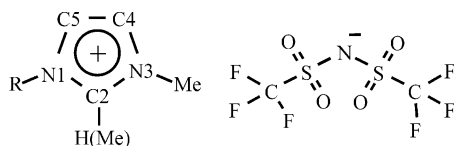
Our results will be of relevance to the interpretation of the various facets of liquid dynamics probed by other experimental methods and vice versa. Among the various techniques, optical Kerr effect (OKE) spectroscopy^{17–19} and time-resolved Stokes shift spectroscopy (TRSS)^{8,20–26} are closely related to dielectric relaxation. OKE spectroscopy probes fluctuations of the polarizability anisotropy. Such experiments have been used to study the picosecond and subpicosecond dynamics of several

* To whom correspondence may be addressed. E-mail: hermann.weingaertner@rub.de.

[†] Ecole Polytechnique Fédérale de Lausanne, Institut des Sciences et Ingénierie Chimiques.

[‡] Physical Chemistry 2, Ruhr-University Bochum.

[§] Institut für Anorganische und Analytische Chemie, Albert-Ludwigs-Universität Freiburg.

**CHART 1: 1-Alkyl-3-methylimidazolium
Bis((trifluoromethyl)sulfonyl)imide**


RTILs,^{17–19} including some bis(triflyl)imides.¹⁷ TRSS spectroscopy probes the time-dependent shift in the fluorescence emission frequency of solvatochromic dyes caused by solvent reorganization after electronic excitation of the dye. In recent years TRSS spectra have been reported for many RTIL/dye couples.^{8,20–26} The underlying solvation dynamics seems to be closely related to the dielectric response of the neat RTILs.^{27,28}

II. Methods

Dielectric Relaxation Spectroscopy. The complex dielectric permittivity (dielectric function) $\tilde{\epsilon}(\nu)$ of an RTIL at frequency ν of the oscillating electric field is given by^{10,29}

$$\tilde{\epsilon}(\nu) = \epsilon'(\nu) - i\epsilon''(\nu) = \epsilon_{\infty} - \Delta\tilde{\epsilon}(\nu) + \sigma/i2\pi\nu\epsilon_0 \quad (1)$$

$$(i^2 = -1)$$

The real part $\epsilon'(\nu)$ reflects dielectric dispersion. $\epsilon'(\nu)$ is usually decomposed into the frequency-dependent contribution $\Delta\epsilon'(\nu)$ and a high-frequency contribution ϵ_{∞} due to electronic and nuclear displacement polarizations. The static dielectric constant ϵ_s is defined as the zero-frequency limit of the dispersion curve. The imaginary part $\epsilon''(\nu)$ reflects dielectric absorption or loss. In addition to the relaxation contribution $\Delta\epsilon''(\nu)$, the measured absorption curve $\epsilon''(\nu)$ involves a diverging low-frequency response proportional to the static (dc) conductivity σ of the sample (“Ohmic loss”). ϵ_0 is the electric field constant. $\Delta\epsilon''(\nu)$ and $\Delta\epsilon'(\nu)$ are interrelated by the Kramers–Kronig relation¹⁰ and do not comprise independent information.

We used a coaxial reflection technique to determine the real and imaginary parts of the complex permittivity of RTILs in the frequency range of 1 MHz < ν < 20 GHz. The frequency range is covered by two apparatus described elsewhere.³⁰

Since this is the first report of this type, it is appropriate to consider in some detail the experimental problems caused by the conductive nature of the liquids. First, high concentrations of mobile charge carriers may generate parasitic polarizations at the interface between the sample and the walls of the sample cells which mimic low-frequency processes. If interfacial effects are absent, a plot of $\nu\epsilon''(\nu)$ against ν approaches a plateau at the low-frequency side of the absorption curve, where only the term $\sigma/i2\pi\nu\epsilon_0$ survives. Interfacial polarizations lead to an increase toward low frequencies. Such effects can be minimized by optimizing the geometry of the specimen cells.

Second, for fluid RTILs the regime of high Ohmic loss is not well separated from the relaxation regime of interest. At the low-frequency side of $\Delta\epsilon'(\nu)$ the term $\sigma/i2\pi\nu\epsilon_0$ increases, eventually rendering the extraction of $\Delta\epsilon''(\nu)$ to be impossible. Moreover, at low frequencies the accurate calibration of the coaxial lines becomes difficult. Typically, calibration relies on a three-point method at each frequency, based on a short circuit, open circuit, and a calibration liquid. The calibration liquids should have a similar dielectric constant and electrical conductivity as the sample under test. For RTILs such standards are not yet available. Reliable calibrations could be obtained in

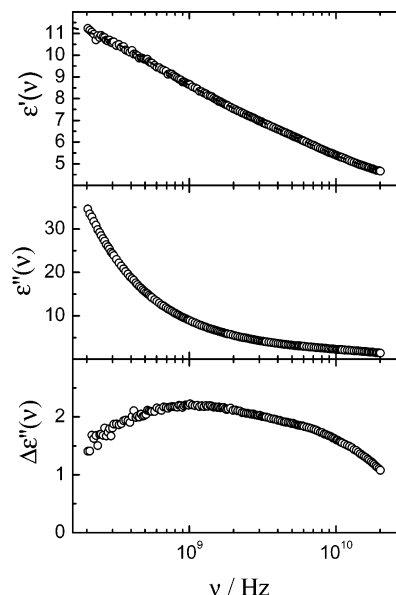


Figure 1. Real part (negative), imaginary part, and conductance-corrected (negative) imaginary part of the complex permittivity of [BuMeIm]⁺[Tf₂N][−] at 298.15 K. The weak high-frequency shoulder of the conductance-corrected absorption curve near 7 GHz should be noted. The corresponding inflections in the dispersion curve are not seen in this large-scale plot.

comparative experiments with nonconductive liquids with static dielectric constants between $\epsilon_s \sim 5$ and 32.³¹

Altogether, the highly conductive nature of the RTILs dictated a lower limit in frequency of about 200 MHz. With some loss in accuracy, our experiments could probably be exploited down to about 50 MHz. However, detailed inspection convinced us that for the salts under test the spectral range above 200 MHz reflected all relaxation components over a sufficiently wide range to characterize the spectra. Therefore the less accurate portion of the spectra below 200 MHz was cut off in data evaluation.

Samples. Sample preparation followed well-established procedures. Briefly, the halide salts of the imidazolium cations were prepared by reacting 1-methylimidazole (Lancaster, 99%, distilled from KOH) or 1,2-dimethylimidazole (Acros, 98%, distilled from KOH) with the corresponding halogenoalkanes, 1-bromoethane (Fluka >98%), 1-chloropropane (Acros, >99%), 1-chlorobutane (Acros, >99%), and 1-bromopentane (Acros, >98%) following literature procedures.^{32,33} Bis((trifluoromethyl)sulfonyl)imides were synthesized from the halides via metathesis in water with LiTf₂N (Fluka, >99%) using published methods.^{14,34} All the ionic liquids were carefully washed with water to avoid the presence of halide impurities and then dried under vacuum (<10 mbar) at 70 °C for several hours, which normally leads to a water content of <100 ppm,³⁵ and actually was found to result in a water content of <5 ppm.

III. Results and Data Evaluation

Experimental Results. We recorded the complex dielectric permittivity of five RTILs at (298.15 ± 0.1) K. Figure 1 shows as a representative example the dispersion curve $\epsilon'(\nu)$ and absorption curve $\epsilon''(\nu)$ of [BuMeIm]⁺[Tf₂N][−] at 200 MHz < ν < 20 GHz. The estimated precision of $\epsilon'(\nu)$ and $\epsilon''(\nu)$ is ± 0.1 . The absolute accuracy, including uncertainties in calibration, is estimated to be better than ± 0.3 . At this level, water contamination and intrinsic impurities of the samples are of no concern.³⁶ In addition, Figure 1 shows the conductance-corrected absorption curve defined by $\Delta\epsilon''(\nu) = \epsilon''(\nu) - \sigma/i2\pi\nu\epsilon_0$.

The dispersion and absorption regimes in Figure 1 are unusually broad. This shape results, in part, from a bimodal structure of the spectrum. In going from [EtMeIm]⁺[Tf₂N][−] to [PeMeIm]⁺[Tf₂N][−], this bimodal structure becomes more pronounced, eventually leading to the high-frequency shoulder in $\Delta\epsilon''(\nu)$, in Figure 1 shown for [BuMeIm]⁺[Tf₂N][−]. In the large-scale plot of Figure 1 the corresponding dispersion curve seems rather featureless, but actually it reveals points of inflection confirming the bimodal structure.

Data Evaluation. The key quantity in spectral parametrization is the time correlation function $\Phi(t)$ of the total electric dipole moment of the sample. Upon Fourier–Laplace transformation, $\Phi(t)$ yields both the real and imaginary parts of the complex permittivity.¹⁰ For multimodal relaxation $\tilde{\epsilon}(\nu)$ is given by

$$\tilde{\epsilon}(\nu) = \epsilon_{\infty} + \sum_k S^{(k)} f^{(k)}(\nu) \quad (2)$$

where $S^{(k)}$ is the relaxation amplitude and $f^{(k)}(\nu)$ the spectral distribution of the k th mode. In the simplest case, each rate process exhibits an exponential decay characterized by the Debye relaxation time τ_D

$$\Phi(t) = \exp(-t/\tau_D) \quad (3)$$

resulting in a spectral function of Lorentzian form

$$f(\nu) = \frac{1}{1 + i2\pi\nu\tau_D} \quad (4)$$

However, bimodal approaches based on eq 4 failed to reproduce the spectra. For example, the widths of the loss peaks were broader than those predicted by eq 4 and in addition their shapes were asymmetrical with a high-frequency tail. Instead of decomposing the signal into further Lorentzians, it seemed more appropriate to apply nonexponential relaxation models.

Many other studies on ionic liquid dynamics have found similar deviations from single exponential relaxation. As repeatedly noted,^{8,18,20–26,37} this nonexponential character is reminiscent of the type of dynamics in glassy liquids,³⁸ suggesting description of the dynamics by a Kohlrausch–Williams–Watts (KWW) stretched exponential representation³⁹

$$\Phi(t) = \exp(-(t/\tau_{\text{KWW}})^p) \quad (5)$$

where $0 < p \leq 1$ is the stretching exponent. It is, however, difficult to apply this expression to experimental data in the frequency domain because the KWW function does not possess an analytical Fourier–Laplace transform. In practice, none of the algorithms for Fourier–Laplace transformation of the KWW function, including a bimodal modification of Provencher's widely used CONTIN algorithm,⁴⁰ were able to cope with the problem of fitting a weak mode below the wing of an intense mode.

A widely used alternative is the empirical Havriliak–Negami (HN) function⁴¹

$$f(\nu) = \frac{1}{\{1 + (i2\pi\nu\tau_{\text{HN}})^{\alpha}\}^{\beta}} \quad (6)$$

$$0 < \alpha \leq 1, \quad 0 < \beta \leq 1$$

which generalizes the Debye equation (4) by two exponents α and β which introduce symmetrical and asymmetrical broadenings, respectively. Equation 6 includes as limiting cases the

symmetrical Cole–Cole (CC) distribution of relaxation times⁴² ($\alpha < 1, \beta = 1$) and the asymmetrical Cole–Davidson (CD) distribution of relaxation times⁴³ ($\alpha = 1, \beta < 1$). For $\alpha = \beta = 1$ the Debye equation is recovered. The HN equation mimics the major features of the KWW distribution, and its parameters can be transcribed into approximate KWW parameters using expressions given by Colmenero and co-workers.⁴⁴

We fitted the real and imaginary parts of the dielectric function by nonlinear regression to eq 6. In all fits σ and ϵ_{∞} were treated as adjustable parameters. Because the conductance correction increases the experimental error of $\Delta\epsilon''(\nu)$ relative to that of $\Delta\epsilon'(\nu)$, we initially focused on data fitting for $\epsilon'(\nu)$ and then ensured that the fit parameters also reproduced $\epsilon''(\nu)$. Later, it became clear that it was a too large a risk to rely on data fitting of the rather featureless dispersion curves which, in parts, provided multiple solutions. Simultaneous fits of the dispersion and absorption curves yielded more robust fits, presumably due to the more structured shape of $\Delta\epsilon''(\nu)$ in comparison to $\Delta\epsilon'(\nu)$.

The data fitted perfectly to a bimodal model with a dominant primary relaxation process denoted by superscript 1, and a weak secondary process at higher frequency (superscript 2). The primary relaxation revealed an asymmetrically broadened spectrum with $\beta^{(1)}$ values of ~ 0.3 to 0.4 and with $\alpha^{(1)}$ values close to unity (typically 0.95 – 1.0). This dominance of the CD over the CC term in eq 6 is also evident from our recent work⁵ on [EtNH₃]⁺[NO₃][−] and from data by Richert and co-workers⁸ for glassy dibutylammonium formate. By virtue of having fewer fitting parameters and achieving more stable fits, we therefore set $\alpha^{(1)} = 1$, for which the HN equation reduced to the CD equation. Note that CD exponents of $\beta^{(1)} = 0.3$ – 0.4 , transcribe to KWW exponents of $p = 0.4$ – 0.5 .⁴⁴

The weak secondary mode proved to be difficult to characterize. A fit based on Debye behavior of the secondary mode ($\alpha^{(2)} = 1, \beta^{(2)} = 1$) provided a perfect representation of the data, but by small variations of the parameters of the primary mode, similarly good fits were obtained with a broad band of exponent values $\beta^{(2)}$ down to $\beta^{(2)} \sim 0.5$. Eventually, a global assessment of the data for all RTILs under test convinced us that for the high-frequency mode a simple Debye-like term was adequate.

Table 1 summarizes the fit parameters for our model consisting of a CD term for the primary relaxation process (1) and a Debye term for the secondary process. The fitted curves were practically indistinguishable from the experimental data. Standard deviations were in the range between $\chi^2 = 0.03$ and 0.07 for both the real and imaginary parts. Table 1 also quotes the static dielectric constants which for a bimodal spectrum are given by $\epsilon_s = \epsilon_{\infty} + S^{(1)} + S^{(2)}$. If all relaxation processes were captured, $\epsilon'(\nu)$ should extrapolate to $\epsilon_{\infty} \cong n^2$, where n is the optical refractive index.¹⁰ For the RTILs under test $n \cong 1.40$ – 1.45 (sodium D line),⁹ i.e., $\epsilon_{\infty} \sim 2.1$. All fits resulted in $\epsilon_{\infty}(\text{fit}) > n^2$. The missing amplitude indicates fast dynamics beyond our frequency cutoff at 20 GHz. Because no perturbations were detected at the high-frequency edge of our spectra, these processes must be well separated on the time scale, presumably with subpicosecond relaxation times.

Table 1 also compiles the fitted conductivities $\sigma(\text{fit})$ extracted from the dielectric spectrum. For comparison, dc conductivity, $\sigma(\text{dc})$, of the samples was measured by a standard conductance bridge. This cross check excludes systematic errors in the evaluation of the permittivity data, for example, caused by hidden interfacial polarizations. We also give in parentheses in Table 1 two conductivity values reported by Watanabe and co-workers.¹⁴ For [EtMeIm]⁺[Tf₂N][−] our result is markedly lower

TABLE 1: Parametrization of the Dielectric Spectra of Imidazolium Bis(triflyl)imides, [RMeIm]⁺[Tf₂N]⁻, at 25 °C by a Bimodal Expression^a

cation	$\tau^{(1)}$, ps	$\tau^{(2)}$, ps	$\beta^{(1)}$	$S^{(1)}$	$S^{(2)}$	e_{∞}	ϵ_s	$\sigma(\text{fit})$, mS cm ⁻¹	$\sigma(\text{dc})$, mS cm ⁻¹
[EtMeIm] ⁺	261	24.2	0.34	7.59	1.43	3.23	12.25	8.45	8.25 (9.04)
[PrMeIm] ⁺	357	25.6	0.38	7.17	1.18	3.45	11.80	4.90	4.77
[BuMeIm] ⁺	482	22.6	0.34	7.46	1.02	3.03	11.52	3.73	3.81 (3.90)
[PeMeIm] ⁺	639	22.2	0.37	7.28	0.89	3.18	11.45	2.68	2.74
[BuMeMeIm] ⁺	593	20.2	0.41	6.66	2.64	2.39	11.45	2.10	2.20

^a The principal relaxation component (1) at low frequencies is parametrized by a Cole–Davidson term given by eq 6 with $\alpha^{(1)} = 1$. The weak secondary component (2) is parametrized by a Debye term given by eq 4. The fitted conductivity $\sigma(\text{fit})$ is compared with the measured dc conductivity $\sigma(\text{dc})$. Values in parentheses are taken from ref 14.

TABLE 2: Parameters Used in the Analysis of the Principal Mode (1)^a

salt	η/cP	$r_{+}/\text{\AA}$	$r_{-}/\text{\AA}$	μ_{+}/D
[EtMeIm] ⁺ [Tf ₂ N] ⁻	37 (22 °C)	3.30	3.81	1.56
[PrMeIm] ⁺ [Tf ₂ N] ⁻	53 (21 °C)	3.49		3.32
[BuMeIm] ⁺ [Tf ₂ N] ⁻	54 (22 °C)	3.60		5.38
[PeMeIm] ⁺ [Tf ₂ N] ⁻	70 (21 °C)	3.73		7.73
[BuMeMeIm] ⁺ [Tf ₂ N] ⁻	118 (22 °C)	3.79		6.15

^a η is the viscosity determined in the present work at the temperature given in parentheses. r is the thermochemical radius of the ions extracted from crystal structures as described in ref 46. μ is the dipole moment of the isolated ion relative to the center of mass. Subscripts “+” and “-” refer to cations and anions, respectively.

than their value. Note that traces of water and halides are expected to enhance the conductivity.

IV. Discussion

A. Spectral Shape. The picosecond to nanosecond dielectric response of the bis(triflyl)imides shows strong deviations from exponential relaxation. Nonexponential dynamics of RTILs on this time scale has also been observed by TRSS^{20–26} and OKE^{18,19} spectroscopy, but there is some controversy about its correct description. In analyzing TRSS spectra, Samanta and co-workers^{20,21} exploited a biexponential relaxation model. In contrast, Maroncelli and co-workers^{22,23} argued that biphasic spectra may be mimicked by a single nonexponential relaxation process. There is common agreement on the existence of further modes on the subpicosecond time scale which in the microwave dielectric spectrum reveal themselves by a missing portion of the dispersion curve.

In the picosecond regime our spectra comprise two discrete modes, but the account for a bimodal spectrum does not remove the necessity to describe the primary relaxation process by strongly nonexponential dynamics. Such a stretching of the relaxation is untypical for simple low-viscosity solvents and strongly reminiscent of glassy dynamics. Many studies of RTILs have found similarly low CD or KWW exponents,^{22–26,37} although the deviations may depend on the type of the experimental probe. Interestingly, more moderate deviations have been observed by us for [EtNH₃]⁺[NO₃]⁻ ($\beta \sim 0.5$)⁵ and by Richert and co-workers for [Bu₂NH₂]⁺[Fo]⁻ ($\beta \sim 0.7$).⁸

B. The Long-Time Diffusive Response. The dominating longest relaxation component is expected to reflect the long-time diffusive response due to collective dipole reorientation.¹⁰ Dipole moments μ_{+} of the ions relative to the center of mass were obtained by us from gas-phase geometries optimized at the (RI)-BP86/SV(P) level using the TURBOMOLE program.⁴⁵ A detailed report of these calculations is given elsewhere.⁴⁶ The dipole moments of the cations in Table 2 are comparable with those of strongly dipolar nonionic species and are large enough to account for the observed relaxation amplitudes $S^{(1)}$. For the [Tf₂N]⁻ anion the literature identifies a conformation with C2

symmetry with a dipole moment of $\mu_{-} \sim 0.59$ D as the relevant dipolar species.¹⁹ On the basis of this observation, the anion would not play a marked role for relaxation. However, the energy surface of the floppy [Tf₂N]⁻ ion is very flat. According to our own calculations,⁴⁶ at least one less symmetric configuration with a dipole moment of $\mu_{-} = 4.59$ D may be relevant.

Quantitative calculations of the relaxation amplitudes are difficult. The familiar theory of dielectric polarization is expected to fail for RTILs because the dipole–dipole interactions between the ions are shielded by the sea of the surrounding charges. At the qualitative level, one expects the amplitude $S^{(1)}$ to be proportional to the square dipole moment, so that the increase of the calculated mass-centered dipole moments along the homologous cation series should result in a large increase in the amplitude $S^{(1)}$. In contrast, our results are practically the same for each salt. However, the dipole moment of charged particles depends on the origin chosen for the atomic coordinates and is thus ill-defined with regard to electrostatic calculations.¹¹ While dipole moments of charged particles are commonly referred to the center of mass, in the light of our data, such mass-centered dipole moments are inadequate. A possible reason is that the increase of the dipole moment in the homologous series does not reflect a substantial redistribution of the charges in the imidazolium ring but mainly results from the displacement of the center of mass when varying the alkyl residue. Giraud et al.¹⁹ circumvented this problem by estimating cation dipole moments from values for similar neutral compounds. Kobrak and Sandalow¹¹ suggested that, in place of the mass-centered dipole moment, the so-called “charge arm” may be used for calculating the orientational polarization. The charge arm is defined by the charge times the distance between the center of mass and center of charge. None of the existing approaches are satisfactory.

Diffusive reorientation should be describable by Stokes–Einstein–Debye (SED) hydrodynamic theory. The SED approach also allows comparison of results from different experiments and for different salts. For a symmetrical ellipsoid rotating in a medium of viscosity η , the reorientation time is given by^{10,47}

$$\tau_{\text{rot}}^L = \frac{6V\eta\xi}{L(L+1)k_{\text{B}}T} \quad (7)$$

where L is the rank of the spherical harmonics associated with the dynamical probe. For dielectric relaxation $L = 1$. The coupling factor ξ depends on the hydrodynamic boundary conditions at the surface of the ellipsoid and on the aspect ratio.

It may be noted that SED theory applies to an exponential relaxation process. Although the reorientation time τ_{rot}^L in eq 7 has often been equated with the mean relaxation times of stretched relaxation time distributions,^{22,23,37} such an approach is by no means evident. Moreover, the dielectric relaxation measures the collective response of all dipoles rather than single-dipole reorientation. Prior to the application of eq 7 the dielectric

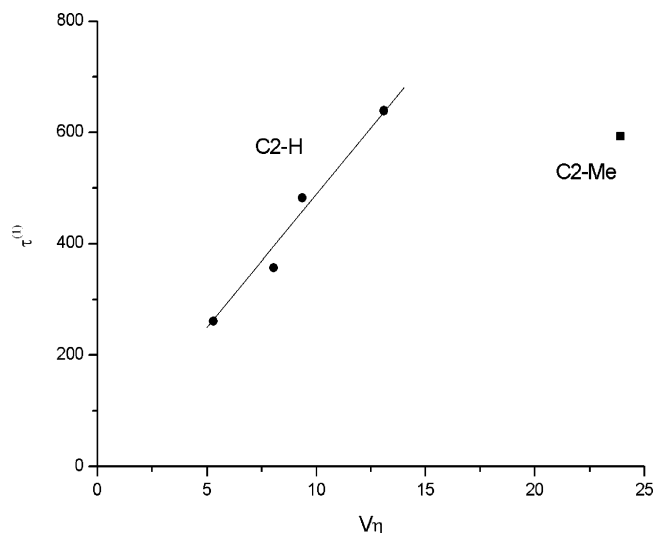


Figure 2. CD relaxation time $\tau^{(1)}$ of the RTILs plotted against the product of volume of the cation (in nm³) times the viscosity (in cP): circles, 1-alkyl-3-methylimidazolium bis(triflyl)imides; square, 1-butyl-2-methyl-3-methylimidazolium bis(triflyl)imide. The solid line is only a guide to the eye.

relaxation times may therefore need correction.^{48,49} Because for RTILs any information on such collective phenomena is lacking, we ignore this correction, as is also explicitly or implicitly done in many interpretations of dielectric relaxation data of nonionic fluids.¹⁰ Note that a similar problem occurs in the evaluation of Kerr effect data of RTILs, where collective effects have been neglected.¹⁸

If hydrodynamics applies, a plot $\tau^{(1)}$ versus the product ηV of the shear viscosity multiplied by the volume of the rotating particle should yield a straight line. Viscosities at ambient temperatures in Table 2 were measured within this work by a standard Ubbelohde-type viscometer and were corrected to 25 °C by assuming an effective activation energy of 25 kJ mol⁻¹ suggested by data in ref 14. The volumes were approximated from the thermochemical radii of the ions in Table 2. These radii were deduced from crystal structures by methods described elsewhere.⁴⁶ The volume of [Tf₂N]⁻ is only slightly larger than those of the cations. Even if the anion's dipole moment were large enough to generate a notable polarization, it would not be possible to discriminate the signal from that of the cations.

Figure 2 shows that $\tau^{(1)}$ behaves in a manner consistent with eq 7, but methyl substitution at carbon C2 destroys this correlation. The viscosity of [BuMeIm]⁺[Tf₂N]⁻ is much larger than that of the parent compound [BuIm]⁺[Tf₂N]⁻, while the dielectric relaxation time is roughly the same. Intuitively, one would expect that hydrogen bond suppression (expected since the most acidic proton is replaced by a methyl group) should lower the viscosity.

While the relaxation times seem to correlate with the viscosity, the quantitative analysis in terms of eq 7 is more subtle. Coupling factors ξ as a function of the aspect ratio of the ellipsoid have been worked out for the limiting cases of stick⁴⁷ and slip⁵⁰ boundary conditions. On the basis of these factors, the hydrodynamic volumes calculated from the relaxation times by means of eq 7 are unreasonably low. If for illustration, we re-express the volumes in terms of radii r of the equivalent spheres, we find for stick conditions values between 1.3 Å for [EtIm]⁺ and 1.6 Å for [PeIm]⁺. For neat liquids the rotating solute has the same size as the surrounding molecules. In this case, slip conditions (i.e., no tangential stress at the surface of the ellipsoid) are known to

give more realistic estimates. Calculations for the slip model depend sensitively on the aspect ratio of the ellipsoid and on the orientation of the dipole vector within the ellipsoid. However, even the most conservative estimates did not result in hydrodynamic radii larger than ~ 2 Å. Our recent data⁵ for [EtNH₃]⁺[NO₃]⁻ imply a similarly low radius.

Neither TRSS spectra nor OKE spectra seem to reveal similarly large anomalies. Direct observation of cation reorientation by ¹³C magnetic relaxation of the ring carbons by Antony et al.³⁷ indicates, however, practically the same deficit of the SED equation (magnetic relaxation is a $L = 2$ property, for which eq 7 implies $\tau_{\text{die}} = 3\tau_{\text{NMR}}$). From a CD-type approach similar to that considered here, Antony et al. typically determine for the stick limit of [BuMeIm]⁺ rotation in [BuMeIm]⁺[PF₆]⁻ a value of $r = 1.2$ Å (albeit at higher temperatures than considered here). This agreement confirms that the long-time diffusive response in the dielectric spectrum reflects ion reorientation. However, it is not clear whether the observed breakdown of eq 7 is a peculiar property of the RTILs or merely a consequence of an inadequacy of the SED equation to deal with broad relaxation time distributions.

C. Ion Pair Orientational Relaxation. There have been many claims for ion pair formation in RTILs, possibly assisted by hydrogen bonds between anions and cationic ring protons. Such statements are, e.g., founded in the analysis of conductance and ion diffusion data.¹⁴ The rationale is that diffusion experiments monitor both free and paired ions, while ions in neutral pairs do not contribute to the conductance. For bis(triflyl)imides such data imply that 40–50% of the ions do not contribute to the conductance.^{14,51} In contrast, it is a common notion that the delocalized charge distribution and low basicity of [Tf₂N]⁻ should minimize the potential for ion pair formation and hydrogen bonding.⁹

If stable at the time scale of molecular reorientation, ion pairs will drive dielectric relaxation in the same way as dipoles in uncharged fluids. Dipolar dumbbells of large ions possess dipole moments larger than 10 D,⁵² so that even a small fraction of dipolar entities should be detectable. These high dipole moments allow, for example, small ion pair concentrations in electrolyte solutions to be traced.^{12,13} One can estimate that 2–3% of ions in long-lived contact ion pairs would account for the observed relaxation amplitudes of $S^{(1)} \sim 7$ and would differ in relaxation time from that of the cation by a factor of 2–3. Our results leave no room for such an interpretation. The rationale is that the observed low-frequency signal is fully explained by ion dynamics, and there is no evidence for any further process hidden below the observed signal. Thus, the ion configurations which escape observation by conductance experiments cannot be stable at the time scale of molecular reorientation. This implies a lifetime of the ion pairs shorter than 100 ps. Previous estimates based on the absence of separate ion pair signals in NMR spectra set an upper limit of the order of microseconds for the lifetime of pairs.¹⁴ It has, however, been known for a long time from work on simple molten salts such as NaCl⁵³ that the correlated motions of oppositely charged ions do not necessarily imply the formation of bound species. Rather, the proximity of the ions in RTILs may give rise to short-time correlations of oppositely charged ions moving in the same direction.

D. The Secondary Mode. The time constant of the secondary process (2) is practically the same for each system, thus not reflecting any viscosity dependence. Strikingly, the longest modes observed in OKE experiments of bis(triflyl)imides by Hyun et al.¹⁷ exhibit time constants of 8–10 ps and are

viscosity-independent as well (the authors correctly note that they obviously miss the diffusive response at longer times). This mode in the OKE spectra is in accordance with the secondary mode observed by us because the time constants obtained by OKE spectroscopy ($L = 2$) transcribe to longer dielectric relaxation times (for diffusive processes $\tau_{\text{rot}}^{L=1} = 3\tau_{\text{rot}}^{L=2}$).

At the present stage, we cannot offer any physical assignment of this secondary mode. Inertial behavior would explain the lack of viscosity dependence but should occur at the subpicosecond time scale. We are not aware of any analogous viscosity-independent dielectric process in homologous series of nonionic fluids, suggesting that this secondary mode is specific to RTILs. Local rate processes associated with the formation of transient ion pairs in the cage of counterions may be an explanation. The residence times of most ions in the cage seem to be longer and comparable to the reorientation time of the ions.^{54,55}

E. High-Frequency Relaxation. Finally, it is interesting to speculate on the origin of the missing high-frequency portion of the spectra. The presence of high-frequency processes is confirmed by several techniques. Fast processes are revealed by OKE spectra,^{17,19} although the modes observed by OKE and dielectric spectroscopy may not be necessarily the same. Recently, TRSS experiments have also been extended to the subpicosecond scale.

With regard to dielectric relaxation itself, evidence for fast dynamics has come from a terahertz spectroscopic study of [EtMeIm]⁺ trifluoromethylsulfonate ([TfO][−]) by Asaki et al.⁵⁶ Their experiments indicate dielectric modes at 2.6 and 0.24 ps, respectively. If the salts considered here would show a mode of notable intensity near 2.6 ps, its wing should be detectable below 20 GHz. Our spectra give no indication for such a process. The missing contribution must be located on a shorter time scale, possibly corresponding to the 0.24 ps process.

Asaki et al.⁵⁶ have attributed the 0.24 ps process to fast hydrogen bond dynamics associated with the C2–H⋯[TfO][−] bond. One of the results of recent quantum-mechanical calculations of the structure and stability of ion pairs¹⁶ is that such hydrogen bonds play a minor role. Neutron scattering studies of the liquid structure of [BuMeIm]⁺[PF₆][−] place the large [PF₆][−] anion above the aromatic ring,⁵⁷ as opposed to a linear C2–H⋯ anion bond assumed by Asaki et al. In fact, it does not need the concept of hydrogen bonding to account for high-frequency librational motions and translational displacements of ions in the cage of counterions. Such motions may, in part, be driven by collective vibrations of the cation lattice with respect to that of the anions. Notably, subpicosecond contributions are also indicated by high-frequency extrapolations of dielectric spectra of glassy ionic conductors. Ngai⁵⁸ presents some evidence, for example from neutron scattering, that these contributions are indeed related to such collective vibrations.

Conclusions

We recorded microwave dielectric spectra of five 1-alkyl-3-methylimidazolium bis(triflyl)imides currently used in many studies as prototypical low-viscosity RTILs. The dynamics of these liquids is complex. The dominant long-time diffusive response at the time scale of several 100 ps can be rationalized by dipolar ion relaxation. The observed relaxation functions are substantially stretched compared with simple exponential rate processes. This similarity of RTIL dynamics to glassy behavior has been repeatedly noted, most recently in a discussion of solvation times of RTIL/dye couples deduced from TRSS spectroscopy.²⁶ In addition, there is a weak viscosity-independent mode at the time scale of 20–30 ps of unclear origin. There

is a striking analogy with a similar mode in OKE spectra. Finally, a missing portion of our dielectric spectra indicates subpicosecond dynamics, as observed by THz spectroscopy and also reflected TRSS and OKE spectroscopy. There is an array of other experimental techniques that highlight different facets of the dynamics of RTILs. The present study helps to establish the similarities and differences in the underlying solvent modes they probe.

Our results constitute a considerable challenge for theory. With regard to the relaxation amplitudes there lacks a detailed understanding of how to describe the charge distribution of an ion by an appropriate dipole moment or a suitable substitute. Moreover, the familiar theory of dielectric polarization is expected to fail for RTILs because the dipole–dipole interactions between the ions are shielded by the surrounding charges. Probably, a suitable interpretation will come from specifically designed molecular dynamics simulations.⁵⁵

Finally, we note that zero-frequency extrapolation of the dispersion curve provides the static dielectric constant ϵ_s of the RTILs. ϵ_s is a key parameter for modeling solvent behavior because many approaches rely on dielectric continuum models for the solvent. For a multimodal relaxation process the static dielectric constant ϵ_s is given by the sum of the relaxation amplitudes $S^{(k)}$ plus ϵ_∞ . The analysis provided makes it possible to attribute the polarization mechanisms generating the dielectric constant. In the RTILs under test the amplitude $S^{(1)}$ due to orientational polarization of the ions accounts for ~80% of the total polarization ($\epsilon_s - n^2$), indicating that in these cases the orientational polarization of the ions represents the major contribution to the dielectric constant.

Acknowledgment. C. Wakai was on leave from the Division of Environmental Research, Institute for Chemical Research, University of Kyoto (Japan). A grant from the Kyoto University foundation is gratefully acknowledged. O. Steinhauser (University of Vienna) and W. R. Carper (Wichita State University) are thanked for many enlightening discussions. M. N. Kobrak (City University of New York) and J. W. Petrich (Iowa State University at Ames) provided reprints.

References and Notes

- (1) Wasserscheid, P.; Keim, W. *Angew. Chem., Int. Ed.* **2000**, 39, 2772.
- (2) *Ionic Liquids in Synthesis*; Wasserscheid, P., Welton T., Eds.; Wiley-VCH: Weinheim, 2003.
- (3) Chiappe, C.; Pierracini, D. *J. Phys. Org. Chem.* **2005**, 18, 275.
- (4) Maroncelli, M.; Fleming, G. R. *J. Chem. Phys.* **1987**, 86, 6221.
- (5) Weingärtner, H.; Knocks, A.; Schrader, W.; Kaatz, U. *J. Phys. Chem. A* **2001**, 105, 8646.
- (6) Wakai, C.; Oleinikova, A.; Ott, M.; Weingärtner, H. *J. Phys. Chem. B* **2005**, 109, 17028.
- (7) See, e.g.: Angell, A. *Chem. Rev.*, **1990**, 90, 523 and references cited therein.
- (8) Ito, N.; Wei, H.; Richert, R. *J. Phys. Chem. B*, in press.
- (9) Bonhôte, P.; Dias, A.-P.; Papageorgiou, N.; Kalyanasundaram, K.; Grätzel, M.; *Inorg. Chem.* **1996**, 35, 1168.
- (10) Böttcher, C. J. F.; Bordewijk, P. *Theory of Dielectric Polarization*; Elsevier: Amsterdam, 1978; Vol. 2.
- (11) See, e.g.: Kobrak, M. N.; Sandalow, N. In *Molten Salts XVI*; Mantz, R. A., Ed.; The Electrochemical Society: Pennington, NJ, 2005.
- (12) Nadolny, H.; Käshammer, S.; Weingärtner, H.; *J. Phys. Chem.* **1999**, 103, 4738.
- (13) Buchner, R. In *Novel Approaches to the Structure and Dynamics of Liquids*; Samios, J., Durov, V. A., Eds.; NATO Science Series II; Kluwer: Dordrecht, 2004; Vol. 133, pp 265–288.
- (14) Tokuda, H.; Hayamizu, K.; Ishii, K.; Susan, M. A. B. H.; Watanabe, M. *J. Phys. Chem. B* **2005**, 109, 6103.
- (15) Dieter, K. M.; Dymek, C. M., Jr.; Heimer, N. E.; Rowang, J. W.; Wilkes, J. S. *J. Am. Chem. Soc.*, **1988**, 110, 2722.

- (16) Tsuzuki, S.; Tokuda, H.; Hayamizu, K.; Watanabe, M. *J. Phys. Chem. B* **2005**, *109*, 16474 and references cited therein.
- (17) Hyun, B.-R.; Dzyuba, S. V.; Bartsch, R. A.; Quitevis, E. L. *J. Phys. Chem. A* **2002**, *106*, 7579.
- (18) Cang, H.; Li, J.; Fayer, M. D. *J. Chem. Phys.* **2003**, *119*, 13017.
- (19) Giraud, G.; Gordon, C. M.; Dunkin, I. R.; Wynne, K. *J. Chem. Phys.* **2003**, *119*, 464.
- (20) Karmakar R.; Samanta, A. *J. Phys. Chem. A* **2002**, *106*, 4447; **2002**, *106*, 6670; **2003**, *107*, 7340.
- (21) Saha, S.; Mandal, P. K.; Samanta, A. *Phys. Chem. Chem. Phys.* **2004**, *6*, 3106.
- (22) Ingram, J. A.; Moog, R. S.; Ito, N.; Biswas, R.; Maroncelli, M. *J. Phys. Chem. B* **2003**, *107*, 5926.
- (23) Ito, N.; Arzhantsev, S.; Maroncelli, M. *Chem. Phys. Lett.* **2004**, *396*, 83.
- (24) Ito, N.; Arzhantsev, S.; Heitz, M.; Maroncelli, M. *J. Phys. Chem. B* **2004**, *108*, 5771.
- (25) Arzhantsev, S.; Jin, H.; Ito, N.; Maroncelli, M. *Chem. Phys. Lett.* **2005**, *417*, 524.
- (26) Chowdhury, P. K.; Sanders, L.; Calhoun, T.; Anderson, J. L.; Armstrong, D. W.; Song, X.; Petrich, J. W. *J. Phys. Chem. B* **2004**, *108*, 10245.
- (27) Halder, M.; Sanders L.; Mukherjee, P.; Song, X.; Petrich, J. W. Submitted for publication in *J. Phys. Chem. A*.
- (28) Song, X.; Chandler, D. *J. Chem. Phys.* **1998**, *108*, 2594.
- (29) Kremer, F.; Schönhals, A. *Broadband Dielectric Spectroscopy*; Springer: Berlin, 2002.
- (30) Oleinikova, A.; Sasisanker, P.; Weingärtner, H. *J. Phys. Chem. B* **2004**, *108*, 8467.
- (31) The reported data refer to calibrations with methanol based on: Barthel, J.; Bachhuber, K.; Buchner, R.; Hetzenauer, H. *Chem. Phys. Lett.* **1990**, *165*, 369. We also compared with other calibration standards based on data in this reference and additional data based on: Buchner, R.; Hefter, G. T.; May, P. M. *J. Phys. Chem. A* **1999**, *103*, 1.
- (32) Cammarata, L.; Kazarian, S. G.; Salter, P. A.; Welton, T. *Phys. Chem. Chem. Phys.* **2001**, *3*, 5192.
- (33) Lancaster, N. L.; Salter, P. A.; Wrelton, T.; Young, G. B. *J. Org. Chem.* **2002**, *67*, 8855.
- (34) Wasserscheid, P.; Sesibg, M.; Korth, W. *Green Chem.* **2002**, *4*, 134.
- (35) Ngo, H. L.; LeCompte, K.; Hargens, L.; McEwen, A. B. *Thermochim. Acta* **2000**, *357/358*, 97.
- (36) We examined the effect of contamination by recording the dielectric spectrum of a sample of [BuMeIm]⁺[Tf₂N]⁻ containing 1000 ppm water. Minor changes in the spectrum were observed which occurred primarily at high frequencies and were consistent with an additional mode due to water relaxation near 10 GHz. Noting that the actual water contamination of the samples is more than two orders of magnitude lower, the residual water content is not of concern.
- (37) Antony, J. H.; Dölle, A.; Mertens, D.; Wasserscheid, P.; Carper, R. W.; Wahlbeck, P. G., *J. Phys. Chem. A* **2005**, *109*, 6676.
- (38) See e.g.: Angell, C. A.; Ngai, K. L.; McKenna, G. B.; McMillan, P. F.; Martin, S. W. *J. Appl. Phys.* **2000**, *88*, 3113.
- (39) Williams, G.; Watts, D. C. *Trans. Faraday Soc.* **1970**, *66*, 80.
- (40) Provencher, S. W. *Comput. Phys. Commun.* **1982**, *27*, 213.
- (41) Havriliak, S.; Negami, S. *J. Polym. Sci.* **1966**, *C14*, 99.
- (42) Cole, K. S.; Cole, R. H. *J. Chem. Phys.* **1941**, *9*, 341.
- (43) Davidson, D. W.; Cole, R. R. *J. Chem. Phys.* **1941**, *19*, 1484.
- (44) Alavarez, F.; Alegria, A.; Colmenero, J. *Phys. Rev. B* **1991**, *44*, 7306.
- (45) See e.g. Arim, M. v.; Ahlrichs, R. *J. Chem. Phys.* **1999**, *111*, 9183.
- (46) Krossing, I.; Slattery, J.; Daguenet, C.; Dyson, P.; Oleinikova, A.; Weingärtner, H. Submitted for publication in *J. Am. Chem. Soc.*
- (47) Perrin, F. *J. Phys. Radium* **1934**, *5*, 497.
- (48) Madden, P.; Kivelson, D. *Adv. Chem. Phys.* **1984**, *56*, 467.
- (49) Weingärtner, H.; Nadolny, H.; Oleinikova, A.; Ludwig, R. *J. Chem. Phys.* **2003**, *120*, 11692.
- (50) Youngren, G. K.; Acrivos, A. *J. Chem. Phys.* **1975**, *63*, 3846.
- (51) Every, H. A.; Bishop, A. G.; MacFarlane, D. R.; Oraedd, G.; Forsyth, M. *Phys. Chem. Chem. Phys.* **2004**, *6*, 1758.
- (52) Typically, a dipolar dumbbell of two oppositely charge hard spheres with centers separated by 4 Å gives rise to a dipole moment of 20 D. Charge delocalization may lower this value. Experimentally determined dipole moments of ion pairs in electrolyte solutions depend on the model used for data evaluation. For systems comprising large organic ions, they are usually larger than 10 D.¹²
- (53) See e.g.: Hansen, J. P.; McDonald, I. R. *Theory of Simple Liquids*, 2nd ed.; Academic Press: New York, 1986; Chapter 10, pp 387–405.
- (54) Morrow, T. L.; Maginn, E. J. *J. Phys. Chem. B* **2002**, *106*, 12807. Note that the MD simulations of [BuMeIm]⁺[PF₆]⁻ reported in this study indicate rotation of the [PF₆]⁻ anion at the 20 ps time scale, as opposed to [BuMeIm]⁺ rotation at the nanosecond scale. This fast anion rotation is, however, a consequence of the high symmetry of [PF₆]⁻. To a first approximation, the rotation of a pseudospherical particle does not displace the surrounding molecules.
- (55) Steinhauser, O.; Schröder, Ch. To be published.
- (56) Asaki, M. L. T.; Redondo, A.; Zawodzinski, T. A.; Taylor, A. J. *J. Chem. Phys.* **2002**, *116*, 7579.
- (57) Hardacre C.; McMath, S. E. J.; Nieuwenhuizen, M.; Bowron, D. T.; Soper, A. K. *J. Phys.: Condens. Matter* **2003**, *15*, S159.
- (58) Ngai, K. L. *J. Chem. Phys.* **1999**, *110*, 10576.